



Effects of dissolved carbon dioxide on growth and vertebral column of hybrid marine grouper (*Epinephelus fuscoguttatus* × *E. lanceolatus*) early advanced larvae

Simon Kumar Das^{a,b,*}, Kumutha Tamil Selvan^a, Noorashikin Md Noor^c, Moumita De^a, David S. Francis^d

^a Department of Earth Sciences and Environment, Faculty of Science and Technology, Universiti Kebangsaan Malaysia, 43600 UKM, Selangor, Malaysia

^b Marine Ecosystem Research Centre (EKOMAR), Faculty of Science and Technology, Universiti Kebangsaan Malaysia, 43600 UKM, Selangor, Malaysia

^c Earth Observation Centre, Institute of Climate Change, Universiti Kebangsaan Malaysia, 43600 UKM, Selangor, Malaysia

^d School of Life and Environmental Sciences, Faculty of Science, Engineering and Built Environment, Deakin University, Geelong, Victoria 3220, Australia

ARTICLE INFO

Keywords:

Aquaculture
Grouper
Intensive culture
Growth
Vertebral column
Osteology

ABSTRACT

This study investigated the effects of different dissolved carbon dioxide (CO₂) concentrations (400, 700, and 1000 ppm) on the growth and vertebral column formation of hybrid tiger grouper × giant grouper (TG × GG) in their advanced larval stage under controlled laboratory conditions for 12 weeks. Growth parameters, including specific growth rate (SGR), survival rate, food consumption (FC), and food conversion rate (FCR), were calculated at the end of the experiment. Vertebral column formation was analysed using X-radiography and osteology methods. The results showed that all growth parameters were significantly affected by CO₂ concentration, with the best performances observed under 400 ppm CO₂. The highest statistically significant ($p < 0.05$) SGR, survival rate, and FC were observed under 400 ppm CO₂, whereas the lowest was observed under 1000 ppm CO₂. The lowest FCR (0.40, $p < 0.05$) was observed in 400 ppm CO₂ and the highest was observed at 1000 ppm CO₂ (0.59, $p < 0.05$). Furthermore, larvae without vertebral column malformations were observed in 400 ppm CO₂, while larvae with small angles of kyphosis were observed in 700 ppm CO₂, and larvae with kyphosis, lordosis, and vertebral compression were observed in 1000 ppm CO₂. Only six spine measurements out of 31 obtained under different CO₂ concentrations were significantly different ($p < 0.05$). Overall, the results suggest that CO₂ concentration plays a crucial role in the growth and vertebral column formation of TG × GG in their advanced larval stage. The optimal CO₂ concentration for the aquaculture of TG × GG in their advanced larval stage was found to be 400 ppm or lower. This study highlights the importance of maintaining optimal CO₂ concentrations to enhance the growth and health of fish in aquaculture systems.

1. Introduction

In fisheries, growth is an important aspect that must be considered to improve fish population management, as it serves as an indicator of fish health in the absence of disturbances in abiotic and biotic factors (Noor et al., 2021). Various environmental factors, including temperature, pH, CO₂ concentration, and calcium carbonate (CaCO₃) saturation, control the distribution, physiological performance, morphology, and behavior of marine invertebrates (Figuerola et al., 2021). Elevated CO₂ levels are predicted to affect important physiological functions in fish, such as

respiration, circulation, and metabolism, which can decrease fish growth rate (Porteus et al., 2018; Noor et al., 2019). The reduction of water pH caused by elevated CO₂ leads to acidification conditions that decrease the blood pH levels of fish, inducing acidosis, which affects fish growth in the long term (Damsgaard et al., 2020). Furthermore, high CO₂ concentrations decrease the pH of animal tissue and can directly affect the efficiency of cellular activities and have potential long-term effects on growth and reproduction (Enzor et al., 2017; Clements and Chopin, 2017). Acidosis can also induce bone demineralization and spinal deformities in fish (Boglione, 2020).

* Corresponding author at: Department of Earth Sciences and Environment, Faculty of Science and Technology, Universiti Kebangsaan Malaysia, 43600 UKM, Selangor, Malaysia.

E-mail address: simon@ukm.edu.my (S.K. Das).

<https://doi.org/10.1016/j.seares.2023.102381>

Received 27 February 2023; Received in revised form 15 April 2023; Accepted 16 April 2023

Available online 18 April 2023

1385-1101/© 2023 Published by Elsevier B.V. This is an open access article under the CC BY-NC-ND license (<http://creativecommons.org/licenses/by-nc-nd/4.0/>).

Elevated CO₂ levels affect the early life stages of multiple taxa, including fish, by reducing shell and skeleton calcification due to a reduction in carbonate availability (Gattuso et al., 1998). Although some fish do not manifest spinal deformities under acidified conditions, certain studies have shown the presence of deformities in the spinal structures of fish during the early stages of fish development (Di Santo, 2019; Narvarte et al., 2020; Mirasole et al., 2021). In light of this, grouper aquaculture is an attractive financial prospect, where the production of hybrid tiger grouper × giant grouper (TG × GG) is dominant. TG × GG is a commercially important hybrid grouper that is extensively exploited in Malaysia due to its fast growth, high survival rate, and simplified larval rearing, making it an attractive prospect for aquaculture (Matpiah et al., 2018; Noor et al., 2019; Das et al., 2021; Luan et al., 2016). Hybridisation techniques in grouper focus on establishing the giant grouper's (*E. lanceolatus*) fast growth rate into other species. However, considering giant grouper is difficult to produce and culture, combining its genetic features into a hybrid allows for better growth (Das et al., 2021). TG × GG is produced by artificially mixing giant grouper milt with tiger grouper eggs. Fast growth, high survival, and simplified larval rearing are advantages of this hybrid. TG × GG is presently the most popular grouper in Hong Kong restaurants (Luan et al., 2016). TG × GG have been the focus of extensive research to determine their advantages in terms of environmental tolerance, disease resistance, and growth. Compared to pure species, they are more adaptable to unfavorable conditions, as per the ocean simulation study (Noor et al., 2019). This will benefit the aquaculture industry by improving the production of important aquaculture species.

The study aims to investigate the effects of different dissolved carbon dioxide (CO₂) concentrations on the growth and vertebral column formation of hybrid tiger grouper × giant grouper (TG × GG) larvae. Specifically, the study aims to determine the growth rate and vertebral column formation of TG × GG larvae under three different CO₂ concentrations (400, 700, and 1000 ppm) using X-radiography and osteology methods. The study also seeks to contribute to the understanding of the effects of elevated CO₂ on early advanced larval fish, as well as the potential impact on the aquaculture industry, particularly in terms of improving the production of important aquaculture species. Ultimately, the results can provide insights into the potential long-term effects of elevated CO₂ on fish growth and development, which could have implications for fisheries management and conservation efforts.

2. Materials and methods

2.1. Sample collection and experimental setup

TG × GG in the early advanced larval stage were collected from a local fish hatchery of Banting Selangor (2°49'0" N, 101°30'0" E), Malaysia. A total of 100 larvae (7 days post hatching [dph]) were collected for experiments. The average length of each fish (7 dph) was 1.5 ± 0.05 cm, and the average weight was 0.95 ± 0.05 g. The larvae were transported to Marine Laboratory of Universiti Kebangsaan Malaysia (UKM) in a large plastic bag containing water and oxygen. The protocols of De et al. (2016) for experimental tank set up and fish rearing were followed with slight modifications. All the experimental tanks were continuously diffused with CO₂-enriched air to produce dissolved CO₂ concentrations of 400 ± 50, 700 ± 100, and 1000 ± 70 ppm.

The aim for these CO₂ concentrations was to reflect the common range of commercial production conditions for this species. Normally CO₂ concentration observed was 400 ppm. In semi-intensive aquaculture, a CO₂ content of 700 ppm is typical, but 1000 ppm is recorded in Recirculating Aquaculture Systems (RAS). Dissolved CO₂ levels can increase in water recirculating aquaculture systems (WRAS) that use pure oxygen supply since the biofilters create free acid, which leads in a significant increase in dissolved CO₂. CO₂ concentration was maintained by using a Hero Tech CO₂ regulator flowmeter with a heater (HPT-GAR-394C-220 V-II), and CO₂ concentration was elevated at a constant rate of

100 ppm day⁻¹ until the experimental CO₂ concentration was reached. The CO₂ concentrations aerated into each experimental tank were controlled by using a scientific-grade pressure regulator and precision needle valve. The concentration of CO₂ in each experimental tank was measured continuously with an in-line infrared CO₂ probe linked to a computer. The computer program Gaslab v2.0.8.14 was used to read the CO₂ concentration level in each tank. After achieving the desired CO₂ concentration, experimental fishes were retained in a flow-through system (water exchange rate of 2 L min⁻¹) in separate 356 L tanks (123 cm × 63 cm × 46 cm) with different CO₂ levels for 12 weeks (Fig. 1). Seawater salinity was monitored by using a Master refractometer (ATA-2352; Atago Co., Ltd., Tokyo, Japan).

In the laboratory, the larvae were evenly distributed among two stocking tanks (1.22 m × 0.46 m × 0.53 m, 284 L in size and capacity). The aquarium tanks were supplied with running artificial seawater at with a salinity level of 30 ppt, temperature of 26.0 ± 0.03 °C, and pH of 6.5 ± 0.5. Oxygen concentration was maintained at >90% saturation. Fish in both holding tanks were fed with pellet diets (Hikari Marine SS Item No. 25210 Kyorin Co. Ltd., crude protein: 48%, crude fat: 8%, crude fiber: 4%, moisture: 10%, ash: 19%, and phosphorus: 1%) similar to those used in hatcheries and acclimated for one week. Once the fish began feeding and defecating properly, they were immediately transferred to the experimental tanks (Mansour et al., 2017).

TG × GG samples with similar body lengths and weights were chosen randomly for the experiment. Fish were randomly distributed into three groups and exposed to three CO₂ levels: 400, 700 and 1000 ppm. Each CO₂ treatment had three replicates, and each replicate tank contained ten fish samples. Thus, three replicates with 30 fish samples for each concentration were obtained.

The larvae were fed twice daily (0800 and 1500 h) with the commercial pellet diet that was previously used during the acclimatization period until satiation. Satiation was determined as the moment when the fish stopped actively feeding and pellets remained at the bottom of the tanks for >2 min (Mazumder et al., 2020). In the evening, unconsumed pellets were removed from the experimental tanks through siphoning. All unconsumed food was removed each night to ensure the appropriate CO₂ condition or environment in each experimental tank and avoid over-feeding. The water quality parameters during the experiment were maintained as follows: temperature of 26.0 ± 0.03 °C, salinity level of 30 ± 0.02 ppt, and pH level of 6.8 ± 0.1. Considering the potential impact of elevated CO₂ concentration on pH reduction, sodium bicarbonate solution was introduced to stabilize the pH levels at approximately 6.8, but it is important to investigate any possible positive or negative impacts of sodium bicarbonate solution on the fish samples. Thus, it is important for the sodium bicarbonate in appropriate concentrations to avoid potential negative impacts on the sample. Water quality parameters were monitored daily at 0900. Temperature was quantified by using a thermometer, whereas pH was measured by using a compact pH meter (LAQUAtwin pH -11). Water was exchanged at the rate of 20% every week to maintain good water quality to reduce the ammonia, nitrite and nitrate concentration in the water excreted by the fish waste and food leftover. The diurnal cycle for the fishes was set at 12 h light and 12 h dark. Body weight and length were recorded every 7 days. The water quality parameters were adequately stable at all the treatment levels of 400, 700, and 1000 ppm, and no significant differences ($p > 0.05$) in all the parameters were observed. These values were found to be within suitable ranges for the culture of TG × GG larvae (Ching et al., 2018) and were maintained throughout the 12-weeks experimental period. In this experiment, 400 ppm was used as indicator for the present oceanic CO₂ levels while 700 and 1000 ppm were marked as the predicted future oceanic CO₂ levels (Pörtner et al., 2019). All laboratory protocols in this study were approved by Animal Ethics Committee of Universiti Kebangsaan Malaysia [approval code no: FST/2016/SIMON/27-JULY/763-JULY-2016-MAY-2017].

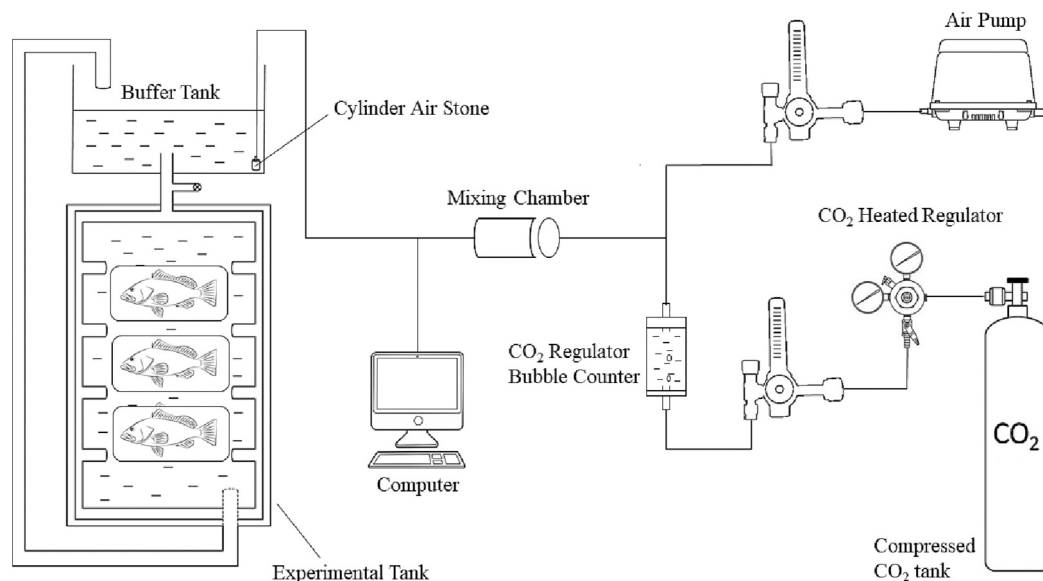


Fig. 1. Experimental tank setup with flow through system (123 × 63 × 46 cm, 356 L in size and capacity).

2.2. Growth

Prior to experimentation, larvae were deprived of food for 2 days prior to being individually weighed and measured under anaesthesia (0.22 mL L⁻¹ α-methyl quinolone Transmore, Nika Trading). Length and weight measurements for SGR calculation were subsequently taken once a week (± 0.1 cm) and electronic balance (A&D, Model-GR-200) (± 0.0001 g). Parameters, such as specific growth rate (SGR), survival rate (%), food consumption (FC), and feed conversion ratio (FCR), were obtained for analysis and growth observation, and calculated as follows:

$$\text{SGR (\% day}^{-1}\text{)} = 100 \times \left(\frac{\text{final weight} - \text{initial weight}}{\text{day}} \right)$$

Survival rate (%) = 100 × (number of live fish at the end of experimental period/number of fish at the beginning of the experiment). The survival rate was computed by dividing the number of live fish at the end of the experiment by the initial number of fish, multiplied by 100.

$$\text{FC (g day}^{-1}\text{)} = \text{g food consumed/day.}$$

FCR (g feed g gain⁻¹) = Amount of feed consumed (g)/wet weight gain (g).

2.3. Vertebral column sampling

X-ray and osteology methods were used to visualize the vertebral columns of TG × GG larvae. The X-ray method was used to visualize the overall vertebral column without using the bone transparency technique and sample staining, whereas the osteology method was used to obtain a detailed image of the vertebral column, including all skeletal elements, bones, and cartilage. The transparency technique, wherein all the tissues in the samples were dissolved and only bony and cartilaginous structures were retained, was used as the osteology method in this study. The transparency technique was performed in reference to Tsandev et al. (2017) with slight modifications.

At the end of the experiment, all remaining fish were humanely killed and fixed in 4% phosphate-buffered formalin (E El-Gamal et al., 2021). After 48 h of preservation, fish were removed from the phosphate-buffered formalin fixative, and their lengths and weights were measured. After weighing, larvae were photographed in the lateral position by using an X-ray machine (Softex, M-60 AC 100 V, 50/60 Hz) connected to a computer for image observation. After imaging, samples were stored in 10% neutral buffered formalin for 24 h. Formalin was chosen as a fixative because it is widely used and can rapidly penetrate the tissues of the samples. The fish samples were fixed to preserve the structural integrity of a specimen for viewing under a microscope.

Through fixation, the tissue and bone of the fish samples were hardened and protected against the deleterious effects of the succeeding histological procedures.

Samples were subsequently stained to reveal skeletal elements. The samples were dissolved in borate buffer (pH of 9.1–9.2) for 24 h, and then in fresh solution for 15 days. The next step after fixation was bleaching, wherein the pigmented surface areas of the samples were bleached in a solution of 0.5% KOH and 1–2 mL L⁻¹ 50% H₂O₂. The specimens were soaked and bleached in this solution for 48–72 h. After bleaching, the samples were rinsed under a weakly running stream of tap water for approximately 5–6 h. Then, the samples were placed in a mixture of saturated sodium borate solution and distilled water with a pH of 8.2–8.3 for 10–12 h. The saturated sodium borate solution was prepared by dissolving dry sodium borate in distilled water at a temperature of 65 °C–70 °C under constant stirring. The solution was allowed to stand for 1–2 days at room temperature until crystals appeared at the bottom of the container.

The samples were then dehydrated slowly and in stepwise manner in an increasing gradient series of alcohol (70% alcohol for 1 day and then in 100% alcohol for 5–12 h) to prevent distortion caused by rapid tissue dehydration and to fully leach out and replace water with alcohol. Following dehydration, the cartilage of the fish samples was stained using Alcian blue solution with absolute ethanol for 24 h at room temperature. Fish samples were then rinsed in distilled water for 30 min and soaked in sodium borate solution for 12 h. Samples were then treated with 1% trypsin solution for 72 h until 25% to 30% of the bone structures became clear and visible. Bones were colorized by staining the samples with Alizarin red with 0.5% KOH. After bone staining, the samples were rinsed with distilled water for 2 h and then immersed in 0.5% KOH and glycerol at a ratio of 2:1 for 10 days. The 2:1 KOH and glycerol solution was replaced with 1:1 KOH and glycerol solution for 2 weeks. Finally, the samples were preserved in glycerol for long term storage.

2.4. Statistical analysis

Statistical analyses of growth parameters were carried using Minitab version 17 (Minitab Inc., Pennsylvania, USA) and OriginLab Corporation. The results were reported as mean ± standard deviation. Prior to analysis, growth parameters, such as SGR, FC, and FCR, were tested for normality and equality of variances. One-way analysis of variance (ANOVA) was used if the data were normally distributed, whereas

Kruskal–Wallis test was performed if the data were not normally distributed to analyze the effects of different CO₂ concentrations on the SGR, FC, and FCR of TG × GG larvae. Tukey’s HSD post hoc test was performed if the equality of variances was met to determine whether a specific group’s means (compared with each other) were different at $p < 0.05$. If the variances were dissimilar, Games–Howell test was carried out. Survival rate was calculated by using a formula, and a line graph was constructed to compare overall percentages under all CO₂ levels.

The standard length and measurements of the spine elements were estimated for each larva from digital photographs via image analysis (Optimas 6.5, Media Cybernetics) (Bashevkin et al., 2020). Spine elements were selected in accordance with two criteria as follows: (1) spine elements were clear and visible in the majority of specimens, and (2) the specimen provided a complete representation and detailed visual of the whole skeleton (Fig. 2, Table 1). Given that the sizes of spine elements are correlated with body size and length, the size of each spine element was regressed against standard length before the analysis. The residuals of this regression among the different CO₂ treatments for each spine element were then compared by using ANOVA. A significance level (α) of 0.05 was used for the analysis.

3. Results

3.1. Growth

The experiment results showed significant differences ($p < 0.05$) in all growth parameters under different CO₂ levels. As CO₂ concentration increased from 400 ppm to 1000 ppm, each growth parameter consistently declined (Table 2). Specifically, SGR decreased significantly ($p < 0.05$, $F = 3098.14$) with increasing CO₂ concentration, with the highest SGR observed in fish at 400 ppm CO₂ (3.37 ± 0.02) and the lowest SGR observed in fish at 1000 ppm CO₂ (0.77 ± 0.03) (Table 2). ANOVA also revealed that FC decreased as CO₂ concentration increased from 400 ppm to 1000 ppm ($p < 0.05$, $F = 313.75$) (Table 2). Interestingly, fish at 400 ppm CO₂ exhibited the highest FCR (1.76 ± 0.06 g day⁻¹), whereas those at 1000 ppm CO₂ had the lowest FCR (1.43 ± 0.05 g day⁻¹). Additionally, ANOVA showed that FCR increased as CO₂ concentration increased from 400 ppm to 1000 ppm ($p < 0.05$, $F = 24.61$) (Table 2). Fish at 400 ppm CO₂ had the lowest FCR of 0.40 ± 0.05 g day⁻¹, while those at 1000 ppm CO₂ had the highest FCR of 0.53 ± 0.05 g day⁻¹.

The survival rate of TG × GG larvae decreased significantly ($p <$

Table 1
Spine measurements at vertebral column with symbols.

Character	Symbol
Standard length	A
First postcranial region of abdominal vertebrae	B
Second postcranial region of abdominal vertebrae	C
First anterior middle region of abdominal vertebrae	D
Second anterior middle region of abdominal vertebrae	E
Third anterior middle region of abdominal vertebrae	F
Fourth anterior middle region of abdominal vertebrae	G
Fifth anterior middle region of abdominal vertebrae	H
Sixth anterior middle region of abdominal vertebrae	I
Seventh anterior middle region of abdominal vertebrae	J
First posterior middle region of neural caudal vertebrae	K
Second posterior middle region of neural caudal vertebrae	L
Third posterior middle region of neural caudal vertebrae	M
Fourth posterior middle region of neural caudal vertebrae	N
Fifth posterior middle region of neural caudal vertebrae	O
Sixth posterior middle region of neural caudal vertebrae	P
Seventh posterior middle region of neural caudal vertebrae	Q
Eighth posterior middle region of neural caudal vertebrae	R
Ninth posterior middle region of neural caudal vertebrae	S
First ural region of neural caudal vertebrae	T
Second ural region of neural caudal vertebrae	U
First posterior middle region of haemal caudal vertebrae	V
Second posterior middle region of haemal caudal vertebrae	W
Third posterior middle region of haemal caudal vertebrae	X
Fourth posterior middle region of haemal caudal vertebrae	Y
Fifth posterior middle region of haemal caudal vertebrae	Z
Sixth posterior middle region of haemal caudal vertebrae	AA
Seventh posterior middle region of haemal caudal vertebrae	AB
Eighth posterior middle region of haemal caudal vertebrae	AC
First ural region of haemal caudal vertebrae	AD
Second ural region of haemal caudal vertebrae	AE
Third ural region of haemal caudal vertebrae	AF

0.05) in a stepwise manner as the CO₂ concentration increased from 400 ppm to 1000 ppm (Fig. 3). The highest survival rate of $80.95 \pm 5\%$ was observed under the 400 ppm CO₂ treatment, while the lowest survival rate of $47.62 \pm 3\%$ was observed under the 1000 ppm CO₂ treatment. The survival rate under 1000 ppm CO₂ was almost half (approximately 50%) that under 400 ppm CO₂, indicating a doubling of mortality of TG × GG larvae under 1000 ppm CO₂.

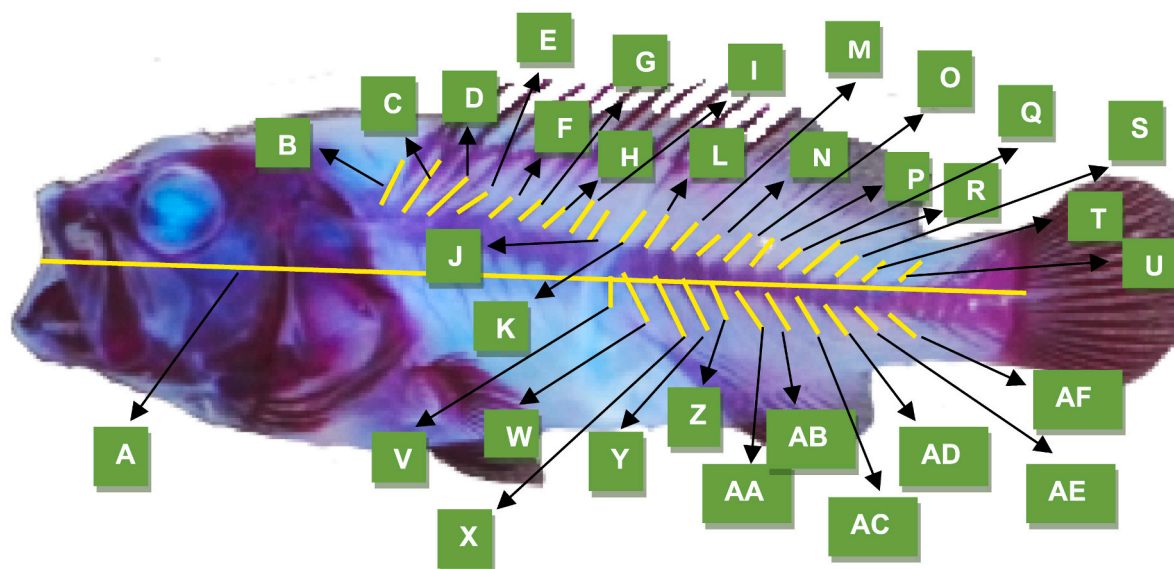


Fig. 2. Photographed of cleared and stained in early advance larvae of TGGG showing the measurements of standard length (A) and 31 spines (B to AF) at vertebral column. Character of each symbol is described at Table 1.

Table 2

Mean squares from analysis of variance that were used to examine the effects of carbon dioxide on SGR (specific growth rate), Weight Gain, FC (feed consumption) and FCR (feed conversion ratio).

CO ₂ Concentration	Mean Squares			
	SGR (% day ⁻¹)	Weight Gain (g)	FC (g day ⁻¹)	FCR
400 ppm	3.37 ^a	17.71 ^a	1.76 ^a	0.40 ^a
700 ppm	1.86 ^b	13.30 ^b	1.69 ^b	0.52 ^b
1000 ppm	0.77 ^c	10.85 ^c	1.44 ^c	0.59 ^c

The lower-case letter ^{a-c} that do not share a letter in each column are significantly different.

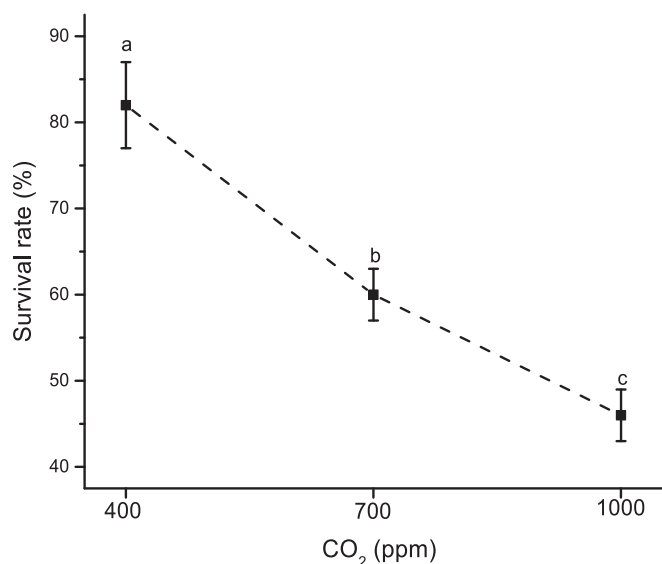


Fig. 3. Survival rate \pm SD of hybrid grouper (TG \times GG) early advanced larvae reared for 12-weeks at different CO₂ concentrations.

3.2. Vertebral column imaging

In order to investigate the effect of different CO₂ concentrations on the formation of vertebral columns in TG \times GG larvae, fish samples exposed to each CO₂ concentration level were X-rayed (Fig. 4). Under 400 ppm CO₂, the vertebral column of TG \times GG larvae (Fig. 4A) exhibited normal growth, formation, and shape. Fish in the 700 ppm CO₂ treatment (Fig. 4B) showed a slight curvature of the precaudal abdominal vertebrae, whereas those in the 1000 ppm CO₂ treatment (Fig. 4C) had irregularly shaped vertebral columns wherein the precaudal abdominal vertebrae were steeply curved upwards (kyphosis), resulting in the malformation of the vertebral column. The formation of skeletal elements was not clearly visible under X-ray. Additionally, differences in the shapes of vertebral columns were observed among the different CO₂ concentrations.

Osteology showed that only fish in the 400 ppm CO₂ treatment exhibited normal vertebral column growth and form. Fish in the 700 ppm CO₂ treatment presented a small angle of kyphosis at the precaudal abdominal vertebrae whilst those in the 1000 ppm CO₂ treatment exhibited a large angle of kyphosis at the precaudal abdominal vertebrae (near the cranium) and lordosis with vertebral compression at the caudal region of the vertebral column (Fig. 5). Statistical analysis was conducted for the 31 spine elements under the different CO₂ concentrations. The measurements for 6 out of 31 spine elements differed under the different CO₂ treatments ($p < 0.05$) (Table 3). The spine elements that differed among CO₂ treatments were the second posterior middle region of the neural caudal vertebrae ($p = 0.02$, $F = 5.22$), the fifth posterior middle region of the neural caudal vertebrae ($p = 0.01$, $F = 6.48$), the sixth posterior middle region of the neural caudal vertebrae ($p = 0.01$, $F = 5.69$), the fourth posterior middle region of the hemal caudal vertebrae ($p = 0.04$, $F = 2.69$), the fifth posterior middle region of the hemal caudal vertebrae ($p = 0.01$, $F = 5.31$), and the seventh posterior middle region of the hemal caudal vertebrae ($p = 0.00$, $F = 1$).

$p = 0.01$, $F = 5.69$), the fourth posterior middle region of the hemal caudal vertebrae ($p = 0.04$, $F = 2.69$), the fifth posterior middle region of the hemal caudal vertebrae ($p = 0.01$, $F = 5.31$), and the seventh posterior middle region of the hemal caudal vertebrae ($p = 0.00$, $F = 1$).

4. Discussion

4.1. Growth

Many recent studies have reported on the negative effects of CO₂ on calcifying organisms, such as corals, crustaceans, and molluscs, but few studies have focused on marine fish under elevated CO₂ conditions, given that marine fish are assumed to be capable of tolerating and surviving elevated CO₂ concentrations (Esbaugh, 2018; Hannan and Rummer, 2018). Studies have shown that some fish species can tolerate elevated CO₂ conditions without any negative effects, whereas others are negatively affected by elevated CO₂ (Clements and Chopin, 2017; Esbaugh, 2018). The present study found that hybrid tiger grouper \times giant grouper (TG \times GG) larvae exhibited reduced growth parameters and increased susceptibility to elevated CO₂ concentrations. However, it is important to note that the study's experimental settings did not encompass all potential CO₂ concentrations, and thus it is possible that some concentrations may have positive effects on fish growth. Fish growth and weight are two important indicators used to assess fish culture conditions (Mota et al., 2019). The SGR of TG \times GG larvae reduced as CO₂ concentration increased from 400 ppm to 1000 ppm, most likely due to the energetic costs incurred by living under elevated CO₂ when overall oxygen consumption remains unchanged (Pörtner et al., 2017). Elevated CO₂ requires TG \times GG larvae to spend extra energy on physiological adaptations, such as acid–base regulation. At the same time, fish also need to spend additional energy on ventilation (Nagelkerken et al., 2021). Marine organisms spend more energy on ventilation in water compared with air-breathing organisms because of the lower percentage of oxygen in seawater than in air and the high viscosity of water. Moreover, as reported by Vernet et al. (2019) under long-term elevated CO₂ conditions, fish undergo negligible respiratory acclimation; this scenario increases the energy expenditure of fish as CO₂ concentrations increase. This result is supported by previous studies within our group, which showed that the growth of TG \times GG juveniles is negatively affected by high CO₂ concentrations of 1000 ppm (Noor et al., 2019). Increased energy expenditure on acid–base regulation and ventilation may affect growth rate because only a small amount of energy is allocated to tissue synthesis. Thus, TG \times GG larvae exposed to 1000 ppm CO₂ might expend little energy on their growth; as indicated by the lowest SGR of 0.77% observed in the 1000 ppm CO₂ treatment. By contrast, TG \times GG larvae under 400 ppm CO₂ likely spend comparatively less energy on acid–base regulation and ventilation, permitting a greater allocation towards growth. The reduction in SGR with the increase in CO₂ concentration might also be attributed to the FC of TG \times GG larvae. The lowest FC was observed under 1000 ppm CO₂. Thus, the reduction in food intake decreased the energy obtained by the fish, which needed to spend additional energy on acid–base regulation. Craig et al. (2017), Steinberg et al. (2017), and Li et al. (2018) also observed reductions in growth rate under similar experimental conditions.

Fish subjected to the 400 ppm CO₂ had the highest FC per day, whilst those in the 1000 ppm CO₂ treatment had the lowest. The FC decreased as the CO₂ concentration was increased, likely due to the unfavorable condition faced by TG \times GG under elevated CO₂. Under heavy CO₂ conditions, such as 700 and 1000 ppm CO₂, fish tended to be passive with minimal movement and did not actively feed, whereas under 400 ppm, fish tended to move and feed actively. As CO₂ concentration increased, the survival rate of TG \times GG larvae decreased. The highest mortality rate was observed under 1000 ppm CO₂ and was almost double the mortality rate under 400 ppm CO₂. Some aquaculture studies have attributed the mortality of fish under elevated CO₂ to nephrocalcinosis, wherein calcareous precipitates form in the kidneys and

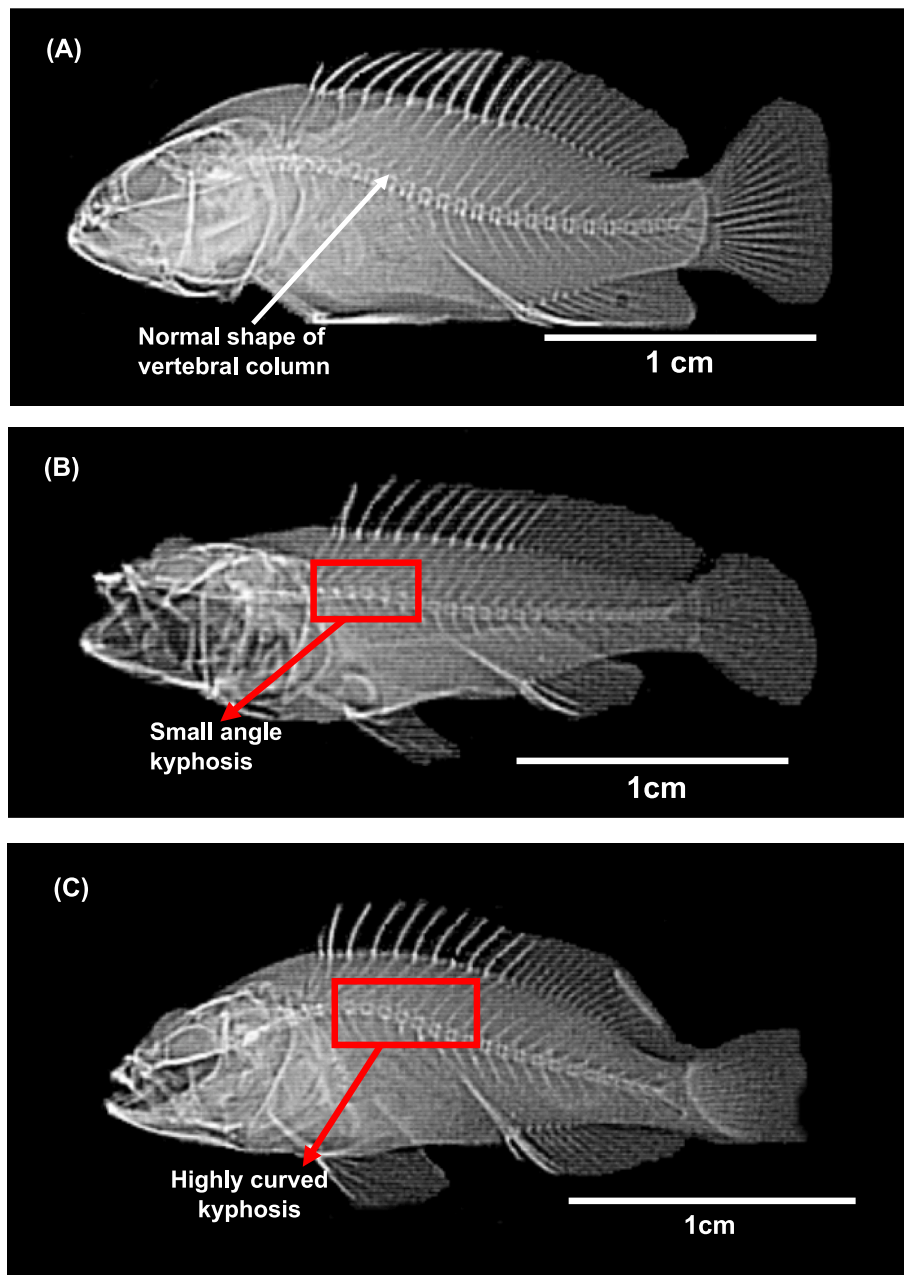


Fig. 4. Skeletal deformities of early advance larvae of hybrid grouper (TG × GG) in different CO₂ concentration using X-ray method (A) 400 ppm: normal formation of vertebral column; (B) 700 ppm: small angle of kyphosis; (C) 1000 ppm: high angle of kyphosis and lordosis.

destroy kidney tubules (Mota et al., 2019; Skov, 2019). While the larvae exposed to 400 and 800 ppm CO₂ showed no significant difference in growth compared to the control group, those exposed to 1000 ppm CO₂ had a significantly lower weight and length. These results are consistent with previous studies that have reported reduced growth rates in fish exposed to high CO₂ levels (Bignami et al., 2013; Munday et al., 2013). The negative impact of high CO₂ levels on fish growth may be due to a reduction in food intake or impaired digestion and metabolism caused by acidosis (Ishimatsu et al., 2008). Additionally, rising CO₂ levels may have indirect effects on fish growth by altering the availability and quality of food sources in the ocean (Fabry et al., 2008). These findings highlight the potential threat of ocean acidification to the growth and survival of fish populations, which can ultimately impact the sustainability of the fisheries industry.

While it is true that many studies have reported on the negative effects of CO₂ on marine organisms, including fish, this study is still novel

in several ways. First, it investigates the effects of elevated CO₂ on a hybrid fish species, specifically the *E. fuscoguttatus* × *E. lanceolatus*, which has not been studied before. Second, this study provides new insights into the energetic costs of living under elevated CO₂ conditions for this fish species, including the additional energy expenditure required for acid-base regulation and ventilation. Third, the study examines the effects of elevated CO₂ on the growth, survival, and feeding behavior of TG × GG larvae, providing valuable information for the aquaculture industry. Finally, this study contributes to the growing body of literature on the effects of elevated CO₂ on marine organisms, which is crucial for understanding and mitigating the impacts of climate change on our oceans. Therefore, despite some overlap with previous research, this study still provides valuable and novel contributions to the field.

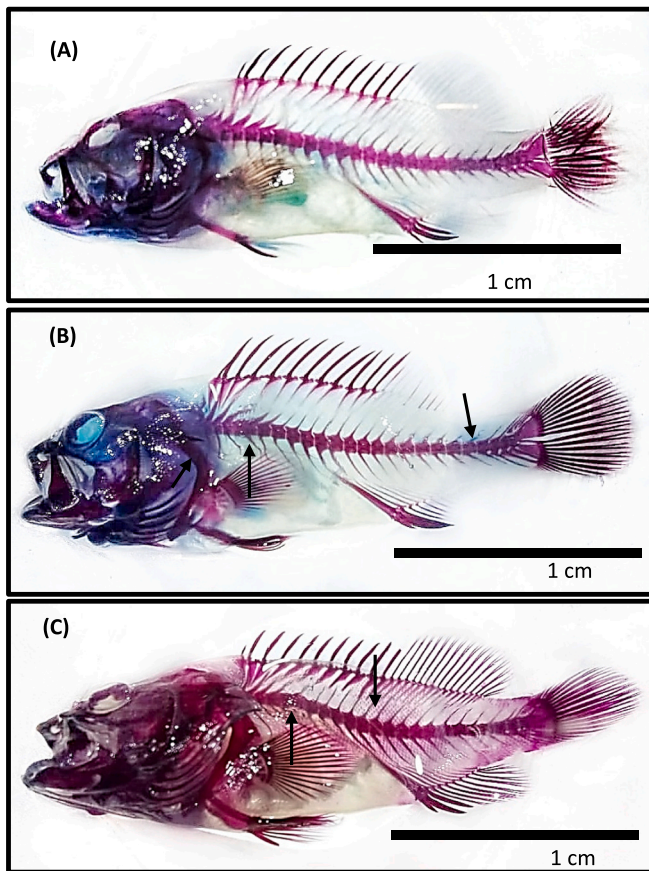


Fig. 5. Skeletal deformities of hybrid grouper (TG × GG) early advanced larvae under the effects of elevated carbon dioxide using osteology method. (A) 400 ppm: Normal formation of vertebral column; (B) 700 ppm: small angle of kyphosis; (C) 1000 ppm: high angle of kyphosis and lordosis.

4.2. Vertebral column

This study demonstrated under simulation that the increasing diffusion of CO₂ in the atmosphere will exert negative effects on TG × GG in the advanced larval stage in terms of not only growth but also vertebral column and skeletal element formation. The malformations found in this study were lordosis, kyphosis, and vertebral compression. However, no cranial deformities, such as ocular migration anomalies, were found. The percentages of vertebral column deformities were high under 1000 ppm CO₂ but low under the other tested CO₂ levels. These results clearly show that fish were not in good welfare following exposure to 1000 ppm CO₂, and were therefore highly susceptible and vulnerable to the negative effects caused by high CO₂. Rising CO₂ was responsible for increasing the percentage of malformations. As the concentration of CO₂ increased, the percentage of malformations in the skeletal elements of TG × GG larvae also increased. Thus, the concentration of CO₂ and percentage of vertebral deformities were correlated. Similar results were observed by [Elsadin et al. \(2018\)](#) and [Baumann et al. \(2018a, 2018b\)](#) who reported that defective skeletogenesis occurs under high CO₂ levels. The findings of the present study, however, contradicted the results of [Crespel et al. \(2017\)](#) who found that the skeletal development of marine fish is not negatively affected by elevated CO₂.

Fish skeletons mainly comprise calcium phosphate in the form of hydroxyapatite, and extensive acid–base regulation may disturb skeletal development ([Lopes et al., 2018](#); [Noor and Das, 2019](#)). Skeletal deformities may negatively affect metabolic and physiological processes in fish in numerous ways. According to in fish, vertebral column curvatures and fin deformities can disturb FC, swimming behavior, and the

Table 3
Analysis of variance of spine elements.

Character	Symbol	One-way ANOVA	
		F-value	p-value
Standard length	A	na	na
First postcranial region of abdominal vertebrae	B	0.00	1.00
Second postcranial region of abdominal vertebrae	C	0.00	1.00
First anterior middle region of abdominal vertebrae	D	0.92	0.44
Second anterior middle region of abdominal vertebrae	E	0.11	0.95
Third anterior middle region of abdominal vertebrae	F	0.00	1.00
Fourth anterior middle region of abdominal vertebrae	G	0.00	1.00
Fifth anterior middle region of abdominal vertebrae	H	0.14	0.94
Sixth anterior middle region of abdominal vertebrae	I	0.00	1.00
Seventh anterior middle region of abdominal vertebrae	J	0.02	0.88
Eighth anterior middle region of abdominal vertebrae	K	0.34	0.57
Ninth anterior middle region of abdominal vertebrae	L	5.22	0.02*
Tenth anterior middle region of abdominal vertebrae	M	0.05	0.82
Eleventh anterior middle region of abdominal vertebrae	N	0.19	0.66
Twelfth anterior middle region of abdominal vertebrae	O	6.48	0.01*
Thirteenth anterior middle region of abdominal vertebrae	P	5.69	0.01*
Fourteenth anterior middle region of abdominal vertebrae	Q	0.36	0.56
Fifteenth anterior middle region of abdominal vertebrae	R	0.11	0.74
Sixteenth anterior middle region of abdominal vertebrae	S	0.02	0.88
Seventeenth anterior middle region of abdominal vertebrae	T	0.01	0.93
Eighteenth anterior middle region of abdominal vertebrae	U	0.70	0.41
Nineteenth anterior middle region of abdominal vertebrae	V	0.15	0.70
Twentieth anterior middle region of abdominal vertebrae	W	0.63	0.43
Twenty-first anterior middle region of abdominal vertebrae	X	0.88	0.36
Twenty-second anterior middle region of abdominal vertebrae	Y	2.69	0.04*
Twenty-third anterior middle region of abdominal vertebrae	Z	5.31	0.01*
Twenty-fourth anterior middle region of abdominal vertebrae	AA	0.31	0.58
Twenty-fifth anterior middle region of abdominal vertebrae	AB	1.00	0.00*
Twenty-sixth anterior middle region of abdominal vertebrae	AC	0.09	0.77
Twenty-seventh anterior middle region of abdominal vertebrae	AD	0.95	0.34
Twenty-eighth anterior middle region of abdominal vertebrae	AE	0.07	0.79
Twenty-ninth anterior middle region of abdominal vertebrae	AF	0.50	0.49
Thirtieth anterior middle region of abdominal vertebrae			
First posterior middle region of neural caudal vertebrae			
Second posterior middle region of neural caudal vertebrae			
Third posterior middle region of neural caudal vertebrae			
Fourth posterior middle region of neural caudal vertebrae			
Fifth posterior middle region of neural caudal vertebrae			
Sixth posterior middle region of neural caudal vertebrae			
Seventh posterior middle region of neural caudal vertebrae			
Eighth posterior middle region of neural caudal vertebrae			
Ninth posterior middle region of neural caudal vertebrae			
Tenth posterior middle region of neural caudal vertebrae			
First ural region of neural caudal vertebrae			
Second ural region of neural caudal vertebrae			
First posterior middle region of haemal caudal vertebrae			
Second posterior middle region of haemal caudal vertebrae			

* p-value < 0.05.

capability for positional maintenance in a current ([Eissa et al., 2021](#)). These effects might account for the reduction in the FC of larvae with the increase in CO₂ levels and directly affected the growth performance of fish. Although the CO₂ concentrations in this study were over-exaggerated to 1000 ppm, the high rate of skeletal deformities under elevated CO₂ might provide insight into how elevated CO₂ may affect the development and performance of TG × GG in the early advanced larval stage. Studies showed that there is a correlation between skeletal deformities and un-inflated swim bladders in larvae of seabream and seabass, which could be due to the oily layer of the water surface, abiotic factors, for example, salinity, water turbulence, light intensity and photoperiod ([Boglione et al., 2013](#); [Elsadin et al., 2019](#)). The deformed skeletal structure in gilthead seabream juveniles could be genetically attributed to an un-inflated swim bladder ([García-Celdrán et al., 2016](#)).

Several past studies have investigated the effects of elevated CO₂ levels on fish development and skeletal structure. [Baumann et al. \(2012\)](#) found that exposure to high levels of CO₂ during the early life stages of clownfish resulted in smaller body size, decreased swimming ability, and abnormal behaviors. Similarly, [Manelli et al. \(2015\)](#) studied the effects of ocean acidification on the development of European sea bass larvae and found that high CO₂ levels caused a significant increase in the incidence of vertebral deformities and abnormalities in the cranial skeleton. In a study on the zebrafish, [Leduc et al. \(2013\)](#) observed skeletal malformations such as spinal curvature and abnormal skull

shape under high CO₂ conditions. Furthermore, Munday et al. (2013) reported that elevated CO₂ levels caused developmental abnormalities in damselfish, including smaller body size and altered behavior. Taken together, these studies suggest that high CO₂ levels can have negative effects on fish development and skeletal structure, leading to impaired survival and reduced fitness. Consequently, these skeletal deformities have deleterious effects on the normal physiological functions of fish through distorting vital processes such as buoyancy, swimming, breathing, and eating, which can ultimately affect the growth rate and survivability of fish.

5. Conclusion

While this study highlights the negative impact of elevated CO₂ on TG × GG larvae during the early advanced larval stage, which resulted in reduced growth and skeletal malformation, it is essential to emphasize the significance of the findings and their implications for future research. The study provides critical guidelines and criteria for future provisional studies on TG × GG larvae or other marine fishes under elevated CO₂ concentrations. Moreover, given that oceanic CO₂ concentrations are rising, there is a need for further long-term studies on the impact of elevated CO₂ concentrations on growth and vertebral column formation, particularly associated with the development of the swim bladder in fish. Such studies are crucial to understanding the potential consequences of increasing CO₂ levels in the ocean, not only for marine fish but also for the wider ecosystem. This study, therefore, contributes to our understanding of the impact of CO₂ on fish larvae and highlights the need for further research in this area. Ultimately, the findings of this study may inform policy decisions aimed at mitigating the effects of rising CO₂ concentrations on marine ecosystems.

Declaration of Competing Interest

The authors declare that there is no conflict of interest exist.

Data availability

Data will be made available on request.

Acknowledgments

This research was funded by Universiti Kebangsaan Malaysia through GGPM-2022-073, and UKM-Sime Darby Foundation Chair in Climate Change grant ZF-2019-003. We would like to extend our appreciation to the staff from the Marine Science Laboratory, Faculty of Science and Technology, UKM for the technical support during the experiments.

References

- Bashevkin, S.M., Christy, J.H., Morgan, S.G., 2020. Adaptive specialization and constraint in morphological defences of planktonic larvae. *Funct. Ecol.* 34 (1), 217–228.
- Baumann, H., Parks, E.M., Murray, C.S., 2018a. Starvation rates in larval and juvenile Atlantic silversides (*Menidia menidia*) are unaffected by high CO₂ conditions. *Mar. Biol.* 165 (4), 1–9.
- Baumann, H., Talmage, S.C., Gobler, C.J., 2012. Reduced early life growth and survival in a fish in direct response to increased carbon dioxide. *Nat. Clim. Change* 2 (1), 38–41.
- Baumann, H., Wallace, R., Tagliaferri, T., Gobler, C.J., 2018b. Large natural pH, CO₂ and O₂ fluctuations in a temperate tidal salt marsh on diel, seasonal, and interannual time scales. *Estuar. Coast. Shelf Sci.* 200, 162–173.
- Bignami, S., Sponaugle, S., Cowen, R.K., 2013. Effects of ocean acidification on the larvae of a high-value pelagic fisheries species, mahi-mahi *Coryphaena hippurus*. *Aquat. Biol.* 18 (3), 281–294.
- Boglione, C., 2020. Skeletal abnormalities. In: *Climate Change and Non-Infectious Fish Disorders*, pp. 54–79.
- Boglione, C., Gavaia, P., Koumoundouros, G., Gisbert, E., Moren, M., Fontagné, S., Witten, P.E., 2013. Skeletal anomalies in reared European fish larvae and juveniles. Part 1: Normal and anomalous skeletogenic processes. *Rev. Aquacult.* 5, S99–S120.
- Ching, F.F., Othman, N., Anuar, A., Shapawi, R., Senoo, S., 2018. Natural spawning, embryonic and larval development of F2 hybrid grouper, tiger grouper *Epinephelus fuscoguttatus* × giant grouper *E. lanceolatus*. *Int. Aquat. Res.* 10 (4), 391–402.
- Clements, J.C., Chopin, T., 2017. Ocean acidification and marine aquaculture in North America: potential impacts and mitigation strategies. *Rev. Aquac.* 9 (4), 326–341.
- Craig, N., Jones, S.E., Weidel, B.C., Solomon, C.T., 2017. Life history constraints explain negative relationship between fish productivity and dissolved organic carbon in lakes. *Ecol. Evol.* 7 (16), 6201–6209.
- Crespel, A., Zambonino-Infante, J.L., Mazurais, D., Koumoundouros, G., Frangkoulis, S., Quazuguel, P., Claireaux, G., 2017. The development of contemporary European sea bass larvae (*Dicentrarchus labrax*) is not affected by projected ocean acidification scenarios. *Mar. Biol.* 164 (7), 1–12.
- Damsgaard, C., McGrath, M., Wood, C.M., Richards, J.G., Brauner, C.J., 2020. Ion-regulation, acid/base-balance, kidney function, and effects of hypoxia in coho salmon, *Oncorhynchus kisutch*, after long-term acclimation to different salinities. *Aquaculture* 528, 735571.
- Das, S.K., Xiang, T.W., Noor, N.M., De, M., Mazumder, S.K., Goutham-Bharathi, M.P., 2021. Temperature physiology in grouper (*Epinephelinae: Serranidae*) aquaculture: A brief review. *Aquac.* Rep. 20, 100682.
- De, M., Ghaffar, M.A., Bakar, Y., Zaidi, C., Das, S.K., 2016. Optimum temperature for the growth form of tiger grouper (*Epinephelus Fuscoguttatus*) × Giant grouper (*E. lanceolatus*) hybrid. *Sains Malaysiana* 45 (4), 541–549.
- Di Santo, V., 2019. Ocean acidification and warming affect skeletal mineralization in a marine fish. *Proc. R. Soc. B* 286 (1894), 20182187.
- E El-Gamal, A.E., El-Sayyad, H., A Sheha, M., O Barakat, R., 2021. Histological and histochemical studies on the ovarian development of the grass carp, *Ctenopharyngodon idella* with special references to atretic phenomena. *Egypt. J. Aquat. Biol. Fish.* 25 (1), 477–492.
- Eissa, A.E., Abu-Seida, A.M., Ismail, M.M., Abu-Elala, N.M., Abdelsalam, M., 2021. A comprehensive overview of the most common skeletal deformities in fish. *Aquac. Res.* 52 (6), 2391–2402.
- Elsadin, S., Nixon, O., Mozes, N., Allon, G., Gaon, A., Kiflawi, M., Tandler, A., Koven, W., 2018. The effect of dissolved carbon dioxide (CO₂) on white grouper (*Epinephelus aeneus*) performance, swimbladder inflation and skeletal deformities. *Aquaculture* 486 (81–89).
- Elsadin, S., Nixon, O., Mozes, N., Allon, G., Gaon, A., Tandler, A., Koven, W., 2019. The effect of dissolved carbon dioxide (CO₂) on the bone mineral content and on the expression of bone-Gla protein (BGP, osteocalcin) in the vertebral column of white grouper (*Epinephelus aeneus*). *Aquaculture* 511, 634196.
- Enzor, L.A., Hunter, E.M., Place, S.P., 2017. The effects of elevated temperature and ocean acidification on the metabolic pathways of notothenioid fish. *Conserv. Physiol.* 5 (1).
- Esbaugh, A.J., 2018. Physiological implications of ocean acidification for marine fish: emerging patterns and new insights. *J. Comp. Physiol. B.* 188 (1), 1–13.
- Fabry, V.J., Seibel, B.A., Feely, R.A., Orr, J.C., 2008. Impacts of ocean acidification on marine fauna and ecosystem processes. *ICES J. Mar. Sci.* 65 (3), 414–432.
- Figuerola, B., Hancock, A.M., Bax, N., Cummings, V.J., Downey, R., Griffiths, H.J., Stark, J.S., 2021. A review and meta-analysis of potential impacts of ocean acidification on marine calcifiers from the Southern Ocean. *Front. Mar. Sci.* 8, 24.
- García-Celdrán, M., Cutáková, Z., Ramis, G., Estévez, A., Manchado, M., Navarro, A., Marfa-Dolores, E., Peñalver, J., Sánchez, J.A., Armero, E., 2016. Estimates of heritabilities and genetic correlations of skeletal deformities and uninflated swimbladder in a reared gilthead sea bream (*Sparus aurata* L.) juvenile population sourced from three broodstocks along the Spanish coasts. *Aquaculture* 464, 601–608.
- Gattuso, J.P., Frankignoulle, M., Wollast, R., 1998. Carbon and carbonate metabolism in coastal aquatic ecosystems. *Annu. Rev. Ecol. Syst.* 29 (1), 405–434.
- Hannan, K.D., Rummer, J.L., 2018. Aquatic acidification: a mechanism underpinning maintained oxygen transport and performance in fish experiencing elevated carbon dioxide conditions. *J. Exp. Biol.* 221 (5) jeb154559.
- Ishimatsu, A., Hayashi, M., Lee, K.S., Kikkawa, T., 2008. Fishes in high-CO₂, acidified oceans. *Mar. Ecol. Prog. Ser.* 373, 295–302.
- Leduc, A.O.H.C., Munday, P.L., Brown, G.E., Ferrari, M.C.O., 2013. Effects of ocean acidification on visual risk assessment in coral reef fishes. *Funct. Ecol.* 27 (4), 947–956.
- Li, J., Haffner, G.D., Paterson, G., Walters, D.M., Burtnyk, M.D., Drouillard, K.G., 2018. Importance of growth rate on mercury and polychlorinated biphenyl bioaccumulation in fish. *Environ. Toxicol. Chem.* 37 (6), 1655–1667.
- Lopes, I.G., Araújo-Dairiki, T.B., Kojima, J.T., Val, A.L., Portella, M.C., 2018. Predicted 2100 climate scenarios affects growth and skeletal development of tambaqui (*Colossoma macropomum*) larvae. *Ecol. Evol.* 8 (20), 10039–10048.
- Luan, G.H., Luin, M., Shapawi, R., Fui, C.F., Senoo, S., 2016. Egg development of backcrossed hybrid grouper between OGGG (*Epinephelus coioides* × *Epinephelus lanceolatus*) and Giant grouper (*Epinephelus lanceolatus*). *Int. J. Aquat. Sci.* 7 (1), 13–18.
- Manelli, F., Gagliano, M., Rossi, R., Sarà, G., 2015. Ocean acidification alters skeletogenesis and gene expression in larval sea bass (*Dicentrarchus labrax*). *Mar. Biol.* 162 (4), 725–737.
- Mansour, O., Idris, M., Noor, N.M., Ruslan, M.S., Das, S.K., 2017. Effects of organic and commercial feed meals on water quality and growth of *Barbonymus schwanenfeldii* juvenile. *AAAL* 10 (5), 1037–1048.
- Matpiah, R., Kadir, A.N.H., Kamaruddin, S.A., Azman, M.N., Ambak, M.A., 2018. Analysis of historical landing data to understand the status of grouper populations in Malaysia. *Malays. Appl. Biol.* 47 (3), 49–58.

- Mazumder, S.K., Abd Ghaffar, M., Das, S.K., 2020. Effect of temperature and diet on gastrointestinal evacuation of juvenile malabar blood snapper (*Lutjanus malabaricus* Bloch & Schneider, 1801). *Aquaculture* 522, 735114.
- Mirasole, A., Scopelliti, G., Tramati, C., Signa, G., Mazzola, A., Vizzini, S., 2021. Evidences on alterations in skeleton composition and mineralization in a site-attached fish under naturally acidified conditions in a shallow CO₂ vent. *Sci. Total Environ.* 761, 143309.
- Mota, V.C., Nilsen, T.O., Gerwins, J., Gallo, M., Ytteborg, E., Baeverfjord, G., Kolarevic, J., Summerfelt, S.T., Terjesen, B.F., 2019. The effects of carbon dioxide on growth performance, welfare, and health of Atlantic Salmon post-Smolt (*Salmo salar*) in recirculating aquaculture systems. *Aquaculture* 498, 578–586.
- Munday, P.L., Jones, G.E., Pratchett, J.M., Ardren, D.R., 2013. Environmental drivers and changes in the prevalence of coral disease in the great barrier reef. *PLoS One* 8, e57345.
- Nagelkerken, I., Alemany, T., Anquetin, J.M., Ferreira, C.M., Ludwig, K.E., Sasaki, M., Connell, S.D., 2021. Ocean acidification boosts reproduction in fish via indirect effects. *PLoS Biol.* 19 (1), e3001033.
- Narvarte, B.C.V., Nelson, W.A., Roleda, M.Y., 2020. Inorganic carbon utilization of tropical calcifying macroalgae and the impacts of intensive mariculture-derived coastal acidification on the physiological performance of the rhodolith *Sporolithon* sp. *Environ. Pollut.* 266, 115344.
- Noor, N.M., Das, S.K., 2019. Effects of elevated carbon dioxide on marine ecosystem and associated fishes. *Thalassas: Int. J. Mar. Sci.* 35 (2), 421–429.
- Noor, N.M., De, M., Iskandar, A., Keng, W.L., Cob, Z.C., Ghaffar, M.A., Das, S.K., 2019. Effects of elevated carbon dioxide on the growth and welfare of Juvenile tiger grouper (*Epinephelus fuscoguttatus*) × giant grouper (*E. lanceolatus*) hybrid. *Aquaculture* 513, 734448.
- Noor, N.M., De, M., Cob, Z.C., Das, S.K., 2021. Welfare of scaleless fish, Sagor catfish (*Hexanemichthys sagor*) juveniles under different carbon dioxide concentrations. *Aquac. Res.* 52 (7), 2980–2987.
- Porteus, C.S., Hubbard, P.C., Uren Webster, T.M., van Aerle, R., Canário, A.V., Santos, E. M., Wilson, R.W., 2018. Near-future CO₂ levels impair the olfactory system of a marine fish. *Nat. Clim. Chang.* 8 (8), 737–743.
- Pörtner, H.O., Bock, C., Mark, F.C., 2017. Oxygen-and capacity-limited thermal tolerance: bridging ecology and physiology. *J. Exp. Biol.* 220 (15), 2685–2696.
- Pörtner, H.O., Roberts, D.C., Masson-Delmotte, V., Zhai, P., Tignor, M., Poloczanska, E., Weyer, N., 2019. IPCC special report on the ocean and cryosphere in a changing climate. In: IPCC Intergovernmental Panel on Climate Change: Geneva, Switzerland, 1(3).
- Skov, P.V., 2019. CO₂ in aquaculture. In: *Fish Physiology*, vol. 37. Academic Press, pp. 287–321.
- Steinberg, K., Zimmermann, J., Stiller, K.T., Meyer, S., Schulz, C., 2017. The effect of carbon dioxide on growth and energy metabolism in pikeperch (Sander *Lucioperca*). *Aquaculture* 481, 162–168.
- Tsandeov, N., Atanasoff, A., Kostadinov, G., Petrova, E., Stefanov, I., 2017. Elaboration of transparent biological specimens for visualisation of developing cartilage and bone structures. *Bulg. J. Vet. Med.* 20 (1), 27–32.
- Vernet, M., Geibert, W., Hoppema, M., Brown, P.J., Haas, C., Hellmer, H.H., Verdy, A., 2019. The Weddell gyre, Southern Ocean: present knowledge and future challenges. *Rev. Geophys.* 57 (3), 623–708.